

Melt growth of bulk Bi₂Te₃ crystals with a natural p–n junction

Cite this: DOI: 10.1039/c3ce42026d

 K. A. Kokh,^{*abc} S. V. Makarenko,^b V. A. Golyashov,^b O. A. Shegai^d
and O. E. Tereshchenko^{bcd}

 Received 7th October 2013,
Accepted 3rd November 2013

DOI: 10.1039/c3ce42026d

www.rsc.org/crystengcomm

Single crystals of Bi₂Te₃ were grown from Bi–Te melts using the modified Bridgman method. It was shown for the first time that solidification of 61 and 62 mol.% Te melts provides a built-in p–n junction on the cleaved plane of as grown crystals without any post growth treatment. The formation of a p–n junction along the growth crystal was explained by Te segregation. Both p- and n-parts of the ingot have shown high carrier concentrations $n \approx p \approx 1 \times 10^{19} \text{ cm}^{-3}$ and high carrier mobility $\sim 10^4 \text{ cm}^2 \text{ V s}^{-1}$ at 4 K. In the transition p–n region, Hall carrier concentration is decreased by two orders of magnitude as a result of intrinsic compensation of carriers.

Introduction

Bismuth telluride based compounds are considered to be among the best thermoelectric materials operating near room temperature.¹ During the last 5 decades, a large amount of research has focused on the study of the Seebeck coefficient in doped Bi₂Te₃ in order to increase the performance of thermoelectric devices. Another issue was to check the type of conductivity provided by a given impurity since it is necessary to have separate blocks of n- and p-type elements.

Satterthwaite and Ure Jr.² provided the details on the phase diagram of the Bi–Te binary system close to the melting point of Bi₂Te₃. The data show that the composition with congruent melting is not a stoichiometric compound but is shifted to the Bi-rich side. That implies that the equilibrium melt for electrically neutral stoichiometric Bi₂Te₃ should be enriched with tellurium. Fig. 1a shows a part of the phase diagram of the Bi–Te system. The “boundary” melt composition, which separates primary crystallization of p- and n-type regions of Bi₂Te₃, was reported to be ~63 mol% Te + 37 mol% Bi.² Later, it was shown that polycrystalline buffer material may be used for changing the composition of bulk Bi₂Te₃ by annealing.³ Incorporation of foreign atoms into the structure of Bi₂Te₃ may also result in the inversion of conductivity. For instance, in ref. 4, it was shown that annealing of bulk p-type

Bi₂Te₃ crystals in selenium vapor transforms the surface layers of the samples to the n-type Bi₂Te_{3-x}Se_x. In that way, a p–n junction between outer n-layers and the internal Se free part of the sample was formed. The same effect was shown for sulfur which leads to the formation of a Bi₂Te₃–Bi₂Te_{3-x}S_x ($x \geq 0.12$) p–n junction by using heat treatment.⁵ Partial substitution of cation by indium also produces the n-type material. This phenomenon was demonstrated for the melt grown Bi_{2-x}In_xTe₃ ($x \geq 0.1$) material in ref. 6.

In recent years, a great deal of attention has been paid to the properties of the tetradymite mineral group showing a novel property of three-dimensional topological insulators.^{7,8} Bismuth telluride is among the compounds of this class; theoretically, its surface state consists of a single nondegenerate Dirac cone, while the bulk state remains insulating.⁹ However, due to their nonstoichiometry, all as grown Bi₂Te₃ crystals are of p- or n-type and therefore exhibit metallic behavior in the bulk. And the resulting intrinsic carriers hamper the study and application of the specific surface states.

Sidestepping of this problem may be carried out by using previous data on transformation of conductivity type in Bi₂Te₃ since the p–n transition should result in the compensation of intrinsic carriers. For instance, the electrical properties can be tuned through a slight increase of Te content in the as grown p-type Bi₂Te₃ crystal by Te-vapor annealing.¹⁰ Another example is the growth of Bi₂(Te,Se)₃ mixed crystals. It was shown that Bridgman solidified Bi₂Te₂Se_{0.995} melt may provide the samples with a positive to negative transition of the Hall coefficient with temperature.¹¹ The same effects as well as domains with different carrier types were found in the crystal grown from the Bi₂Te₂Se melt.¹²

Although the adjustment of tellurium pressure is very promising for the growth of stoichiometric Bi₂Te₃ thin

^a Sobolev Institute of Geology and Mineralogy, SB RAS, 3, Koptyuga Ave., Novosibirsk 630090, Russia. E-mail: k.a.kokh@gmail.com; Fax: +7 383 33066392

^b Novosibirsk State University, 2, Pirogov Str., Novosibirsk 630090, Russia. E-mail: k.a.kokh@gmail.com; Fax: +7 383 33066392

^c Tomsk State University, 36, Lenina Ave., Tomsk, 634050, Russia.

E-mail: k.a.kokh@gmail.com; Fax: +7 3822 529585; Tel: +7 3822 529852

^d Rzhanov Institute of Semiconductor Physics, SB RAS, 13, Koptyuga Ave., Novosibirsk 630090, Russia. E-mail: teresh@isp.nsc.ru; Fax: +7 383 3304475

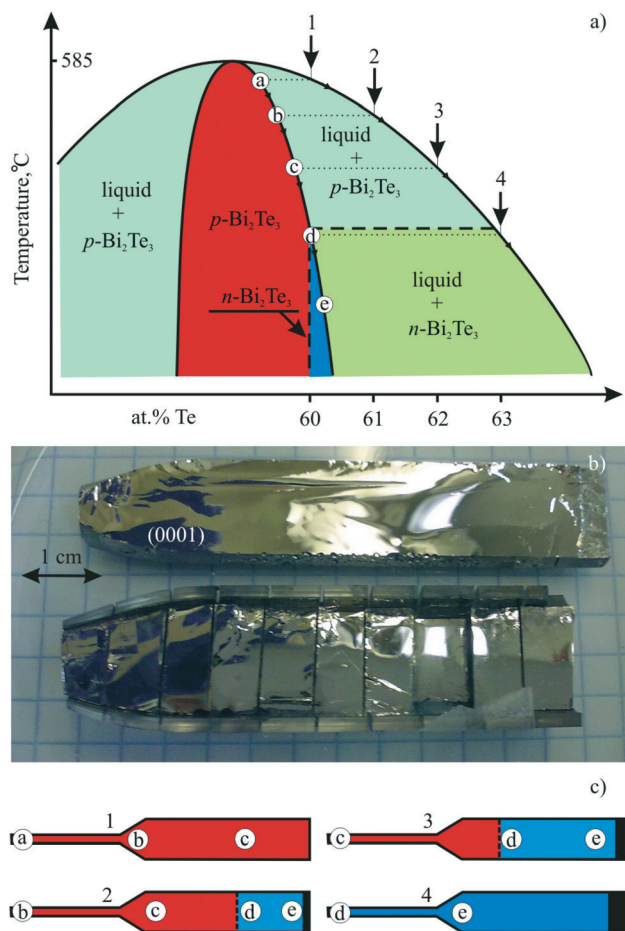


Fig. 1 (a) Schematic phase diagram of a Bi-Te section close to the Bi_2Te_3 composition, based on the data of ref. 2; (b) single crystal of Bi_2Te_3 cleaved along (0001); (c) localization of the p-n junction depending on melt composition.

films,¹³ this work aimed to show that a stoichiometric domain may also be formed in the bulk single crystals of bismuth telluride due to the natural process of Te segregation.

Experimental

In this work, the experiments on crystallization of Bi_2Te_3 from various melts in the Bi-Te system were carried out. The starting compositions were chosen as 60, 61, 62 and 63 mol% of tellurium (Fig. 1a). At the melting point of Bi_2Te_3 (858 K), the saturated pressure of elementary Bi and Te does not exceed the strength of the 1.5 mm wall ampoule. Therefore, the charges were prepared by direct alloying of elementary components of 5 N purity in quartz ampoules. The synthesis furnace was heated at the rate of 50 K per hour up to 870 K, and after 10 hours of melt homogenization, it was switched off. Growth of single crystals was performed in carbon coated ampoules with a 4 cm tip for geometrical selection of spontaneous microcrystals. The inner diameter of the ampoules was 14 mm, while that of the tip was 4 mm. Both synthesis and growth ampoules were sealed under a residual pressure of $\sim 10^{-4}$ torr. Crystal growth procedure was carried out using

the modified Bridgman technique^{14–16} with an $\sim 10 \text{ K cm}^{-1}$ temperature gradient at the front of crystallization. After pulling the ampoule at a rate of 5 mm per day, the furnace was switched off.

As grown ingots had a single crystalline structure and were split into two parts along the cleavage plane {0001} oriented along the growth direction. One part of each crystal was cut perpendicular to the growth axis into 4–5 mm samples for electrophysical measurements (Fig. 1b). The Hall resistance R_{yx} and the resistance R_{xx} were measured in the Hall bar geometry using a standard six-probe method on rectangular samples on which the contacts were made with indium at the perimeter. The magnetic field was swept between $\pm 4 \text{ T}$ at fixed temperatures and was always applied perpendicular to the films.

Results and discussion

It is known that sufficiently slow directional crystallization occurs under conditions of quasi-equilibrium.¹⁷ It means that any solidification step takes place under thermodynamic equilibrium at the front of crystallization, while diffusion in solid phase is slow enough to maintain composition inhomogeneities. If the composition of the solidifying phase does not match the initial melt, the latter will follow *the liquidus* line on the phase diagram while the solid phase will be represented by *the solidus*, the sequence of compositions being in equilibrium with the liquid phase at each step of crystallization. Based on the data of ref. 2 and Fig. 1, it can be concluded that solidification of the Bi_2Te_3 melt over-enriched with Te may provide either p- or n-type Bi_2Te_3 crystals. And the governing factor is the initial composition of the melt. It should be noted that our data on the phase diagram are in good agreement with those of ref. 2.

Fig. 1c illustrates the relationship between the initial melt composition and the resulting distribution of components in the crystals. Crystallization of melt with 60 mol% of Te (composition 1) provides the Bi_2Te_3 ingot with the a \rightarrow b \rightarrow c sequence of compositions. With a further decrease in temperature, the projection of composition 1 intersects the solidus line of p- Bi_2Te_3 which means that crystallization is completed at this stage. This is confirmed by the fact that both initial and end parts of the crystal grown from composition 1 show p-type conductivity. Composition 4 (63 mol% Te) falls onto the part of liquidus which is in equilibrium with n- Bi_2Te_3 . Crystallization of that sample starts with compositions d \rightarrow e... and ends with the eutectic aggregate $\text{Bi}_2\text{Te}_3 + \text{Te}$ (shown by the black region at the end of samples 2, 3 and 4). The samples from that ingot showed n-type conductivity.

A combination of both p- and n-type conductivities was found in the crystals grown from compositions 2 and 3. According to the phase diagram, at the first stage of solidification, the melts are in equilibrium with Bi_2Te_3 of p-type (b-composition for melt 2 and c-composition for melt 3). However, crystallization of Bi_2Te_3 results in the gradual increment of Te concentration in the melt. When the concentration

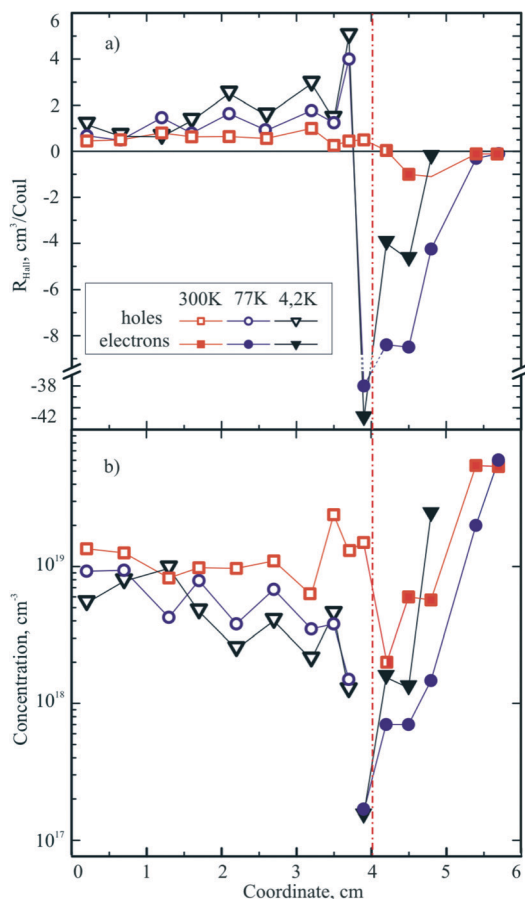


Fig. 2 Change of Hall coefficients (a) and carrier concentration (b) along crystal 2 at 300 (squares), 77 (circle) and 4 K (triangle). The current and Hall voltage were parallel to the cleavage plane, and the magnetic field was perpendicular to the cleavage plane.

exceeds 63 mol% of Te, the composition of Bi_2Te_3 at the front of crystallization corresponds to an n-type crystal. Thus, a natural p–n transition in the Bi_2Te_3 crystal can be formed by means of tellurium segregation during crystal growth. A position of this boundary in the crystal is determined by initial melt composition. Obviously, the transition in crystal 2 is located closer to the end of the ingot than in the case of crystal 3.

The Hall measurements at the bottom and top parts of the crystals showed opposite signs of Hall coefficients R_H , demonstrating the presence of p- and n- regions in crystals 2 and 3. Fig. 2 shows the changes of the Hall coefficients R and carrier concentration at 300, 77 and 4 K along the crystal with composition 2. In contrast to $\text{Bi}_2(\text{Te},\text{Se})_3$ crystals,^{11,12} we observe a positive-to-negative transition of R_H with temperature only in the region of the p–n junction with a width of about 300 μm . At a distance of over 200 μm from the p–n junction, Hall measurements show the domination of one type of carrier in these Bi_2Te_3 crystals. The samples from initial parts 0–2 cm show metallic behavior with small positive Hall coefficients (1 to 3 $\text{cm}^3 \text{K}^{-1}$) leading to a weak temperature-dependent p-type carrier concentration $p = (5\text{--}10) \times 10^{18} \text{ cm}^{-3}$ at 4.2 K. At the top part of the crystal, a similar metallic-like behavior was observed for n-type

carriers ($n \approx 10^{19} \text{ cm}^{-3}$). A large carrier concentration and its weak temperature-dependent behavior indicate that these parts of the material are heavily doped by acceptors or donors. The temperature dependence of the conductivity confirms the metallic character of these p- and n-separated parts. In the vicinity of the p–n junction, the Hall coefficient changes sign and increases to $-42 \text{ cm}^3 \text{K}^{-1}$ at low temperatures, and the carrier concentration decreases by two orders of magnitude (down to 10^{17} cm^{-3}). In both p- and n-parts of the crystal, the mobility shows a high average value of $10^4 \text{ cm}^2 \text{V s}^{-1}$ at 4 K which reaches the maximum at $7 \times 10^4 \text{ cm}^2 \text{V s}^{-1}$ in the n-type region located close to the p–n junction. Note, finally, that similar to the Bi_2Se_3 (0001) surface,^{18,19} the cleaved Bi_2Te_3 (0001) surface showed high quality and stability to oxidation after a month of air exposure.

Conclusions

By using the modified Bridgman method, single crystals of Bi_2Te_3 were grown with the built-in p–n junction formed along the crystal growth axis and perpendicular to the cleavage (0001) plane. In the grown crystals, the p–n junction was observed at all temperatures and its location depended on the initial Bi/Te ratio in the melt. The changes in the Bi/Te ratio during the growth process and, as a consequence, the compensation for the p-type majority carriers are caused by the Te segregation to the top part of the boule. The availability of such material is quite promising since the compensated bulk volume should show no electric conduction. Also, the existence of a lateral p–n junction promises to extend the variety of spintronic applications such as the topological p–n junction and the dual gate TI device.^{20,21}

Acknowledgements

Support from RFBR 12-02-00226 and 13-02-12110 is acknowledged.

Notes and references

- X. A. Yan, B. Poudel, Y. Ma, W. S. Liu, G. Joshi, H. Wang, Y. Lan, D. Wang, G. Chen and Z. F. Ren, *Nano Lett.*, 2010, **10**, 3373.
- C. B. Satterthwaite and R. W. Ure Jr., *Phys. Rev.*, 1957, **108**, 1164.
- J. P. Fleurial, L. Gaillard, R. Triboulet, H. Scherrer and S. Scherrer, *J. Phys. Chem. Solids*, 1988, **49**, 1237.
- P. Lostak, J. Horak, R. Novotny and J. Klikorka, *J. Mater. Sci.*, 1987, **6**, 1469.
- J. Horak, P. Lostak, L. Koudelka and R. Novotny, *Solid State Commun.*, 1985, **55**, 1031.
- L. Jansa, P. Lostak, J. Sramkova and J. Horak, *J. Mater. Sci.*, 1992, **27**, 6062.
- H. Zhang, C.-X. Liu, X.-L. Qi, X. Dai, Z. Fang and S.-C. Zhang, *Nat. Phys.*, 2009, **5**, 438.
- K. Miyamoto, A. Kimura, T. Okuda, H. Miyahara, K. Kuroda, H. Namatame, M. Taniguchi, S. V. Eremeev, T. V. Menshchikova,

- E. V. Chulkov, K. A. Kokh and O. E. Tereshchenko, *Phys. Rev. Lett.*, 2012, **109**, 166802.
- 9 Y. L. Chen, J. G. Analytis, J.-H. Chu, Z. K. Liu, S.-K. Mo, X. L. Qi, H. J. Zhang, D. H. Lu, X. Dai, Z. Fang, S. C. Zhang, I. R. Fisher, Z. Hussain and Z.-X. Shen, *Science*, 2009, **325**, 178.
- 10 Y. S. Hor, D. Qu, N. P. Ong and R. J. Cava, *J. Phys.: Condens. Matter*, 2010, **22**, 375801.
- 11 Sh. Jia, H. Ji, E. Climent-Pascual, M. K. Fuccillo, M. E. Charles, J. Xiong, N. P. Ong and R. J. Cava, *Phys. Rev. B: Condens. Matter Mater. Phys.*, 2011, **84**, 235206.
- 12 J. L. Mi, M. Bremholm, M. Bianchi, K. Borup, S. Johnsen, M. Sodergaard, D. Guan, R. C. Hatch, P. Hofmann and B. B. Iversen, *Adv. Mater.*, 2013, **25**, 889.
- 13 J. Krumrain, G. Mussler, S. Borisova, T. Stoica, L. Plucinski, C. M. Schneider and D. Grützmacher, *J. Cryst. Growth*, 2011, **324**, 115.
- 14 K. A. Kokh, Yu. M. Andreev, V. A. Svetlichnyi, G. V. Lanskii and A. E. Kokh, *Cryst. Res. Technol.*, 2011, **46**, 327.
- 15 K. A. Kokh, B. G. Nenashev, A. E. Kokh and G. Yu Shvedenkov, *J. Cryst. Growth*, 2005, **275**, e2129.
- 16 K. A. Kokh, V. N. Popov, A. E. Kokh, B. A. Krasin and A. I. Nepomnyaschikh, *J. Cryst. Growth*, 2007, **303**, 253.
- 17 *Crystallization technology handbook*, ed. A. Mersmann, 2001, Marcel Dekker Inc., New York, p. 832.
- 18 V. A. Golyashov, K. A. Kokh, S. V. Makarenko, K. N. Romanyuk, I. P. Prosvirin, A. V. Kalinkin, O. E. Tereshchenko, A. S. Kozhukhov, S. V. Ereemeev, S. D. Borisova and E. V. Chulkov, *J. Appl. Phys.*, 2012, **112**, 113702.
- 19 V. V. Atuchin, V. A. Golyashov, K. A. Kokh, I. V. Korolkov, A. S. Kozhukhov, V. N. Kruchinin, S. V. Makarenko, L. D. Pokrovsky, I. P. Prosvirin, K. N. Romanyuk and O. E. Tereshchenko, *Cryst. Growth Des.*, 2011, **11**, 5507.
- 20 J. Wang, X. Chen, B. F. Zhu and S. C. Zhang, *Phys. Rev. B: Condens. Matter Mater. Phys.*, 2012, **85**, 235131.
- 21 J. E. Yazyev and S. G. L. Moore, *Phys. Rev. Lett.*, 2010, **105**, 266806.